International Journal of Applied Pharmaceutics

ISSN- 0975-7058 Vol 17, Issue 4, 2025

Original Article

HPTLC QUANTIFICATION OF 4, 4'-METHYLENE BIS (2,6-DI-TERT-BUTYL PHENOL) IN FLAX MICROGREEN EXTRACTS AND ITS ANTICANCER POTENTIAL AGAINST PROSTATE CANCER

MUDASSIR LAWAL[1,2], NEETA RAJ SHARMA[3], AWADHESH KUMAR VERMA[4*], IBRAHIM HAMZA KANKIA[5], VETRISELVAN SUBRAMANIYAN[6], GURMEEN RAKHRA[1]

[1]Department of Biochemistry, School of Bioengineering and Biosciences, Lovely Professional University, Phagwara, Punjab, India. [2]Department of Biochemistry and Molecular Biology, Federal University Dutsin-Ma, Katsina-Nigeria. [3]Department of Biotechnology, School of Bioengineering and Biosciences, Lovely Professional University, Phagwara, Punjab, India. [4]Department of Bioinformatics, School of Bioengineering and Biosciences, Lovely Professional University, Phagwara, Punjab, India. [5]Department of Biochemistry, Faculty of Natural and Applied Sciences, Umaru Musa Yar'adua University, Katsina-Nigeria. [6]Department of Medical Sciences, School of Medical and Life Sciences Sunway University, No. 5, Jalan Universiti, Bandar Sunway-47500 Selangor Darul Ehsan Malaysia

*Corresponding author: Awadhesh Kumar Verma; *Email: dradverma@gmail.com

Received: 16 Apr 2024, Revised and Accepted: 23 Apr 2025

ABSTRACT

Objective: This research aimed to evaluate the antioxidant activity of methanolic extract of flax microgreens (MEFM), to identify and quantify 4,4'-Methylenebis (2,6-Di-tert-butylphenol) [4,4'-M(2,6-DTBP)] using GC-MS and HPTLC, and to assess its inhibitory activity against prostate cancer.

Methods: *In vitro* antioxidant activity was determined by 2,2-Diphenyl-2-picryl-hydrazyl (DPPH) scavenging activity. 4,4'-M(2,6-DTBP) was identified and quantified by Gas Chromatography-Mass Spectrometry (GC-MS) and High Performance Thin Layer Chromatography (HPTLC) analysis. The docking simulation had been carried out in PyRx 0.8 software. Toxicity studies were performed using ADMETlab 3.0 and ProTox 3.0 prediction tools, respectively. The cytotoxic effects and induction of apoptotic cell death by MEFM and 4,4'-M(2,6-DTBP) on PC-3 cell lines were assessed by MTT(3-(4,5-dimethylthiazol-2-yl)-2,5-diphenyltetrazolium bromide) and Annexin V apoptosis assays, respectively.

Results: The HPTLC fingerprint confirmed the presence of 4,4'-M(2,6-DTBP) in the MEFM and indicated its existence in high content. 4,4'-M(2,6-DTBP) exhibited the highest binding energies (−17.1 kcal/mol) and favorable interactions against prostate cancer target proteins. The Absorption, Distribution, Metabolism, Excretion, and Toxicity (ADMET) prediction studies revealed that this 4,4'-M(2,6-DTBP) compound had low toxicity and distinct metabolic properties. The MEFM showed strong growth inhibition against PC-3 (IC_{50}: 377.5 µg/ml), whereas 4,4'-M(2,6-DTBP) exhibited weak growth inhibition (IC_{50}: 2324.78 µg/ml). The Annexin V assay revealed that the MEFM and 4,4'-M(2,6-DTBP) significantly increased total apoptosis to 41.03% and 22.86%, respectively. In early apoptotic cells, the MEFM and 4,4'-M(2,6-DTBP) caused 40.9% and 19.5% cell death, while in late apoptotic cells, cell death was found to be 0.13% and 3.36%, respectively.

Conclusion: The extract and its bioactive compound demonstrate anticancer potential, but *in vivo* studies are required to further evaluate efficacy, metabolism, and toxicity in a living system.

Keywords: ADMET, Antioxidants, Anti-prostate cancer, Flax microgreens, HPTLC, Molecular docking

DOI: https://dx.doi.org/10.22159/ijap.2025v17i4.53939 Journal homepage: https://innovareacademics.in/journals/index.php/ijap

INTRODUCTION

Prostate Cancer (PCa) means a cancer that exists within the prostate gland, which is a part of the male reproductive system. It is also called prostate carcinoma. PCa has both hereditary and environmental risk factors and remains the second leading cause of cancer-related deaths in men (after lung cancer) [1]. According to the Surveillance, Epidemiology, and End Results (SEER) Cancer Statistics Review 2024, prostate cancer is ranked with second highest estimated death rate (10.92%) among men across the world [2]. Medicinal plants are widely used by human beings worldwide, and in recent years, they have played a major role in the treatment of diseases [3]. Different plant extracts have been traditionally utilized to minimize the cancer medication's adverse effects for their efficacy, ease of preparation, affordability, and accessibility. Flax is a versatile plant and belongs to the family *Linaceae*. The botanical name for flax is "*usitatissimum*," which means "the most useful" in Latin [4]. They may help to reduce the risk of heart disease and also help in improving digestion, type 2 diabetes, and the treatment and prevention of cancers [5, 6]. The bioactive compounds, such as flavonoids, lignans, and omega-3 fatty acids, including alpha-linolenic acid (ALA), present in flaxseeds have been shown to possess anti-carcinogenic effects by inhibiting the key regulatory proteins [7]. Previously, multiple experimental studies have shown that dietary flaxseeds lower prostate cancer risk by significantly delaying the proliferative effect and lowering the Prostate-Specific Antigen (PSA) in wistar rats [8].

Polyphenols are naturally occurring phenols having many other health benefits apart from their antioxidant activity [9]. Previous studies have indicated that polyphenol-rich diets prevent the development of certain diseases, including diabetes mellitus, cancers, neurodegenerative diseases, and cardiovascular diseases [10, 11]. A compound known as 4,4'-Methylenebis (2,6-DI-tert-butylphenol) [4,4'-M (2,6-DTBP)] is a member of polyphenols synthesized in plants through a shikimate/phenylpropanoid pathway, which leads to the formation of different polyphenolic compounds involved in plant defense, antioxidant activity, and other biological functions [12, 13]. A number of studies have demonstrated a vast array of biological activities of 2,4-Di-tert-butyl-butyl phenol (2,4 DTBP), a derivative of 4,4'-M(2,6-DTBP), including antibacterial, anti-inflammatory, antifungal, antioxidant, and anti-cancer activities [14-16]. Several findings have verified the anti-prostate cancer effects of flax and flaxseeds, but no research has yet explored the anti-proliferative properties of flax microgreens and its bioactive compound 4,4'-M(2,6-DTBP) in prostate cancer therapy. Hypothetically, flax microgreens and their bioactive compounds may exhibit anticancer properties by inhibiting prostate cancer growth through molecular interactions and cytotoxic effects. As the researcher has been interested in exploring the health benefits of flax/flaxseeds, the objectives of this study involve the evaluation of the antioxidant activity of methanolic extract of flax microgreens (MEFM), identification and quantification of 4,4'-M(2,6-DTBP) by Gas Chromatography-Mass Spectrometry (GC-MS) and High-Performance Thin Layer Chromatography (HPTLC) analysis, molecular docking simulation to find out the interaction of the

inhibitory effect of 4,4'-M(2,6-DTBP) by binding with the protein target of prostate cancer, and the *in vitro* cytotoxic effect of MEFM and 4,4'-M(2,6-DTBP) on PC-3 cell lines. Such knowledge gained from this research would not only contribute to the delineation of the intervention potential of flax microgreens but also offer a framework for an in-depth understanding the mode of action of this phytocompound for PC treatment. Also, it will contribute to surging investigations about plant-derived sustainable cancer treatments that support the United Nations Sustainable Development Goals (UNSDGs).

MATERIALS AND METHODS

Chemicals

4,4'-M(2,6-DTBP) and DPPH were purchased from Sigma-Aldrich (St. Louis, MO, USA). Dulbeccos Eagles Minimum Essential Medium (DMEM), Foetal Bovine Serum (FBS), Phosphate Buffered Saline (DPBS), Trypsin-EDTA solution, and MTT reagent were all purchased from MP Biomedicals, Germany. Dimethyl Sulfoxide (DMSO), Propidium Iodide (PI), Methanol (HPLC grade) and HPTLC Silica Gel 60 F254 Plates were purchased from Merck (Darmstadt, Germany). Annexin V-AbFlourTM 488 Apoptosis Detection Kit (KTA0002) was purchased from Abbkine Scientific Co., Ltd (Abbkine, Inc USA).

Flax microgreens collection and authentication

Flax seeds were purchased from a local Market at, Phagwara, Punjab, India. The flax microgreens used in this study were grown by sowing the seeds in cocopeat at Lovely Professional University's (LPU) Hi-Tech Polyhouse in Phagwara, Punjab, India. Its identity was authenticated by a Professor in Plant Taxonomy, Kebbi State University of Science and Technology Aliero (KSUSTA) Dr. Dharmendra Singh, with voucher specimen number (KSUSTA/PSB/H/Voucher No: 657) deposited in the herbarium of the institute.

Flax microgreens extraction

50 g of powdered flax microgreens were subjected to extraction with 250 ml of methanol using the cold maceration method. The sample was kept in a sealed container and allowed to macerate for 24 hrs. After maceration, the mixture was filtered through Whatman filter paper Grade 1 [17] to remove the residues. The filtrate was concentrated with a rotary evaporator and stored at −4 degrees Celsius for future analysis [18].

DPPH scavenging assay

A DPPH scavenging assay was used to estimate the extracts' free radical scavenging activity [19-21]. The methanol was used to prepare a 0.1 mmol DPPH solution, and 1.6 ml of methanol extract at various concentrations (62.5, 125, 250, 500, and 1000µg/ml) was added to 2.4 ml of DPPH solution. The mixture was thoroughly vortexed and kept in the dark at room temperature for 30 min. Using spectrophotometry, the mixture's absorbance was measured at 517 nm. The following formula was to determine the percentage DPPH scavenging activity:

$$\% \text{ DPPH scavenging activity} = \frac{\text{Absorbance of control} - \text{Absorbance of the sample}}{\text{Absorbance of control}} \times 100$$

The IC_{50} was estimated by plotting the inhibition percentage against the concentration. The experiment was repeated in triplicate [20, 22].

GC-MS analysis

The sample was analysed using a Shimadzu (GCMS-TQ8040 NX) Gas Chromatograph connected with a Perkin Elmer Turbo Mass 5.1 mass detector fitted with Elite – 1 fused silica capillary column (30 m × 0.25 mm ID × 0.25 µm), functional in Central Instrumentation Facility Lab (CIF) at LPU, Phagwara, Punjab, India. The oven temperature was initially set to 50 °C for 3 min, then rose up to 300 °C at 10 °C/min, and was maintained for 8 min. Temperature of the injector was set at 250 °C, injector size 1 uL neat, with split ratio of 1:10, and carrier gas (Helium) was used at flow rate of 1.02 ml/min. The mass spectrometry (MS) ion source and interface were maintained at 240^{0}C and 310^{0}C, respectively; the mass spectra were taken at 70eV with a mass scan range of 34-600(m/z). The MS started at 4 min, and ended at 37 min, with solvent cut time of 4 min. GC-MS solution software was used to analyse the data. The mass spectra of the identified compounds were compared with those in the National Institute of standards and technology (NIST) and WILEY libraries [23].

HPTLC analysis

Standard 4,4'-M(2,6-DTBP) preparation

1 mg/ml of stock was prepared by dissolving the 6 mg of 4,4'-M(2,6-DTBP) in 6 ml of methanol. Consequently, stock solution (1 ml) was added to methanol (10 ml) to obtain 0.1 mg/ml of 4,4'-M(2,6-DTBP) [24].

Test samples (extract) preparation

To achieve 1 mg/ml of MEFM solution, 10 mg of extract was added into methanol (10 ml). The resultant solution was then filtered with a membrane filter (0.22 mm) [25].

HPTLC setup conditions and instrumentation

HPTLC was conducted on a silica gel 60 f 254 (3.0 × 10 cm; Merck, Germany) HPTLC plate. The plate was kept in an automatic development chamber with a mobile phase consisting of ethyl acetate: toluene: formic acid in a 5:4:0.2 (V/V/V%) ratio. Using an automated spray applicator with a 100 µl** syringe, 6.0 µl** of both extract and the standard solution of 4,4'-M(2,6-DTBP) with a concentration of 1 mg/ml was applied to the plates in the form of 8.0 mm bands at the rate of 150 nl/s. The CAMAG-Linomat IV was used for sample application, and its settings were as follows: application rate of 150 nl/s, band length of 8.0 mm, distance between bands 10 mm, distance from the bottom of the plate measuring 10.0 mm, and distance from the plate side edge of 5 mm. WIN CATS program version 1.4.6.2002 was used to densitometrically evaluate the bands using CAMAG TLC Scanner 3. The following were the settings for the scanner: (Scanning rate: 20 mm/s; Slit dimension: 6.00 x 0.45 mm; Mode: absorption/reflection; monochromator bandwidth: 30 nm at an optimum wavelength of 515). The retention factor (Rf) value was calculated as:

$$\text{Rf} = \frac{\text{Distance traveled by the compound}}{\text{Distance traveled by the solvent front}}$$

The peak area corresponding to the Rf value of the standard was recorded, and the peak of the isolated component from the extract was compared to that of the standards for identification. Also, the calibration curves were used to determine the target compound's concentration [26, 27].

In silico studies

Docking and biomolecular interactions

The software known as PyRx, which employs Vina and Autodock 4.2, was utilized to analyze the protein-ligand interaction through a molecular docking simulation [28, 29]. The 2D (2-dimensional) structure of 4,4'-M(2,6-DTBP) and the Food and Drug Administration (FDA) approved drug were procured from the chemical structure database (PubChem) in .SDF format and converted to .PDBQT format prior to docking [30-32]. The target proteins' 3D (3-dimensional) structures were retrieved from the PDB's website (http://www.rscb.org/pdb) [33], and the binding site was subsequently predicted using a grid box analysis [28]. Proteins and ligands were prepared and docked using PyRx as previously described by Lawal *et al.* [18] and Aiswariya and Satya, [34]. Upon the docking search completion, the protein-ligand interactions was analyzed using ligand interaction profiler (PLIP) software [35, 36]. The strength of ligand binding was measured as a negative score in kcal/mol [37]:

$$\mathbf{K_i = e^{-\Delta^{DG/RT}}}$$

Where:

Ki = Inhibition constant (measure of binding affinity).

ΔG = Gibbs free energy change of binding (in Joules or kcal/mol)

Universal gas constant (R) = (1.985x 10^{-1} kcal/mol/K)

Temperature (T) = (298.1.5 K)

ADME/T properties prediction

Online softwares (ProTox-3.0 and ADMETlab 3.0) were used to predict the Absorption, Distribution, Metabolism, Excretion, and Toxicity (ADMET) parameters, toxicology of the studied compounds [38], and violations of Lipinski's rule of five (LRO5) and Veber's rule (VR) as described by Lawal et al. [18], and only one variation is accepted in the case of variables [39].

***In vitro* studies**

Cell viability assay

The PC-3 cell lines were obtained from the National Centre for Cell Science (NCCS), Pune. The cells were cultured in DMEM containing 10% FBS, 200 µl of the cell suspension (about 10,000 cells) was placed in 96-well plates, and the plates were kept in a 37 °C and 5% CO2 atmosphere for 24 hrs. The test samples were solubilized using DMSO, diluted into culture medium containing serum-free medium. After 24 hrs, spent mediums were replaced with mediums containing test samples in various concentrations (62.5, 125, 250, 500, and 1000µg/ml) and incubated for 24 hrs in CO_2 incubator (37 °C and 5% CO_2)

After the time period, the drug-containing media was aspirated, and 100 µl of MTT (5.0 mg/ml) in PBS was added to each well and incubated for 4 h at 37°C. To solubilize the dark blue formazan crystals, 100 µl of DMSO was added and mixed gently. After solubilization at room temperature, the absorbance was read at 570 nm and also at 630 nm using a microplate reader. The IC_{50} was made from the dose-response curve [40, 41]. The growth inhibition was calculated using the formula below:

$$\text{Growth inhibition} = \frac{\text{OD control - OD treated}}{\text{OD Control}} \times 100$$

Annexin-V apoptosis assay by flow cytometry

PC-3 cells were cultured in a 6-well plate with a seeding density of 3 x 10^5 cells per 2 ml. Cells were incubated in a CO_2 incubator overnight at 37° C for 24 hrs. Following this, the spent medium was discarded, and the cells were rinsed with 1 ml of 1X PBS. The cells were then treated with 2 ml of culture medium containing the necessary concentration of experimental test compounds and cultured for 24 hrs. Some of the wells were left untreated as a negative control. At the end of the treatment, the cells were harvested directly into centrifuge tubes and washed with 500 µl PBS. The PBS was removed and then incubated with 200 µl trypsin-EDTA at 37 °C for 3-4 min. The culture medium was then returned to their original wells while collecting the cells into the centrifuge tubes. Afterward, the tubes were centrifuged at 300 x g for 5 min at 25 °C. The supernatant was cautiously decanted, washed twice with PBS, and PBS was decanted completely. Cells were resuspended in a concentration of 1 x 10^6 cells per ml in 1X Binding Buffer. 100 µl of the solution containing 1 x 10^5 cells was added into a 5 ml culture tube, and subsequently, 5 µl of AbFlour 488 Annexin V to the mixture was added and incubated for 15 min at 25 °C in the dark with gently vortex. 400 µl of 1X Binding buffer and 2 µl of PI were added to each tube, followed by gentle votexing. The samples were subjected to flow cytometry analysis as soon as the PI was added [42, 43].

Statistical analysis

The *GraphPad Instat 3* software and Microsoft Excel spreadsheet were used to analyze statistical significance of each data set; the results are shown as Mean±SD. Non-significant (ns) is defined as a P value>0.05, *P ≤ 0.05, **P ≤ 0.01.

RESULTS AND DISCUSSION

DPPH scavenging activity

This is a widely used technique for determining a plant extract's potential for antioxidant activity. DPPH donates hydrogen ions to molecules in their oxidized form, acting as a free radical scavenger or antioxidant [44, 45]. The result of the DPPH scavenging activity of MEFM is presented in fig. 1. The extracts exhibited a concentrated dependent increase in scavenging activity. At a 1000 µg/ml concentration, the MEFM exhibited higher DPPH radical scavenging activity of 84.2%. Though MEFM exhibited DPPH radical scavenging activity, it is significantly (p<0.001) less effective than ascorbic acid at all tested concentrations. The current results agreed with the report by Alachaher *et al.* [46], which indicates that the DPPH scavenging capacity of methanolic and butanolic extracts of *L. usitatissimum* was 93.1% and 96.2%, respectively, at 800 µg/ml. According to the results of Hanaa *et al.* [47], the aqueous methanol (70%) extract of flaxseeds exhibited a maximum level of inhibition of 62.10%, which is significantly higher than the current findings. This might be attributed to the fact that aqueous methanol (70%) is more polar and it can extract a good amount of phenolic compounds.

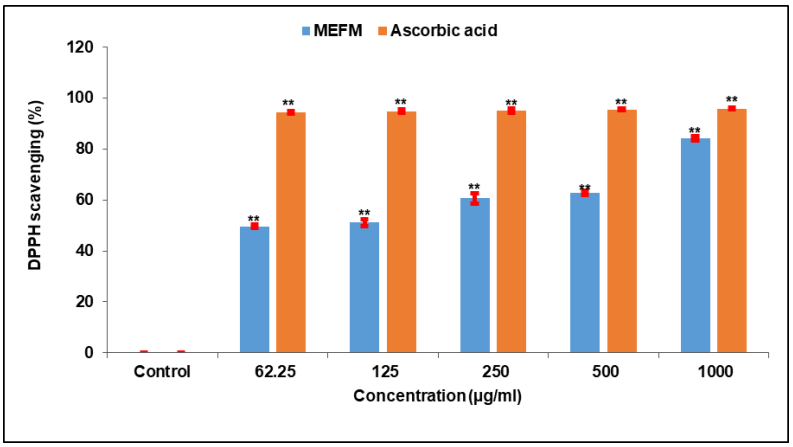

Fig. 1: DPPH scavenging activity of MEFM compared to ascorbic acid control. Data are presented as mean and standard deviation (mean±SD) of three replicates mean values (bar graphs), Standard deviation (vertical lines), Asterisk (**) above the bars is statistically significance (*P* ≤0.001)

GC-MS analysis and bioactive compound selection process

GC-MS analysis results revealed that the MEFM contains several phytocompounds that exhibit various phytochemical activities, as reported by Lawal *et al.* [18]. We selected the bioactive compounds based on their abundance in the extract. Table 1 presents the bioactive compounds with higher peak area (>2.0%) along with their molecular formula, molecular weight (MW), and retention time (RT). Pre-docking screening was conducted; all the selected phytocompounds were docked against the six (6) druggable targets

of prostate cancer, with their binding energies recorded in table S1 (see supplementary material). 4,4'-M(2,6-DTBP) shows the highest binding energies with a range of −10.7 to −17.1 Kcal/mol across the target proteins. This compound was selected for further study.

Table 1: Flax microgreen's bioactive compounds with highest percentage

S. No.	RT	Compound CID:	Compound names	Molecular formula	Molecular weight	Peak area (%)
1	21.824	985	n-Hexadecanoic acid	$C_{16}H_{32}O_2$	256.42	4.27
2	23.460	17161	2,5-Di-*tert*-butyl-1,4-benzoquinone	$C_{17}H_{24}O_3$	276.4	4.33
3	23.756	64947	(2R,3S,4S,5R,6S)-2-(hydroxymethyl)-6-methoxyoxane-3,4,5-triol	$C_7H_{14}O_6$	194.18	13.01
4	24.091	54725318	L-Ascorbic acid, 6-octadecanoate	$C_{24}H_{42}O_7$	442.6	5.21
5	24.510	637775	3,5-Dimethoxy-4-hydroxycinnamic acid (Sinapinic acid)	$C_{11}H_{12}O_5$	224.21	3.21
6	25.911	5280435	Phytol	$C_{20}H_{40}O$	296.5	3.22
7	27.872	10494	Oleanolic acid	$C_{30}H_{48}O_3$	456.7	2.40
8	29.695	191964	bis(2-propylpentyl) benzene-1,2-dicarboxylate	$C_{24}H_{38}O_4$	390.6	4.19
9	31.038	8372	4,4'-Methylenebis (2,6-DI-tert-butylphenol)	$C_{29}H_{44}O_2$	424.7	2.74
10	32.875	638072	Squalene	$C_{30}H_{50}$	410.7	4.62

*RT: Retention time

HPTLC analysis

The optimum mobile phase development for 4,4'-M(2,6-DTBP) separation was achieved by using the solvent system of ethyl acetate: toluene: formic acid (5:4:0.2 V/V/V%) as shown in the HPTLC fingerprint (fig. S1; see supplementary material). The HPTLC analysis of MEFM has shown the presence of 4,4'-M(2,6-DTBP) in a higher concentration. The chromatograms and peak tables were generated by scanning at 515 nm. The densitometry graph (fig. 2) illustrates the peaks for track 1, representing 4,4'-M(2,6-DTBP) (standard), and track 2, representing 4,4'-M(2,6-DTBP) from MEFM. The HPTLC fingerprint revealed the abundance of this compound in MEFM with an area percentage of 100% (table 2). Fig. 3 represents both the 3D and overlay of the chromatograms of all tracks. The Rf values, peak area, peak height, and percentage area of the compound are depicted in table 2. The specificity of the 4,4'-M(2,6-DTBP) compound in the extract was confirmed by comparison between the extract's Rf values and those of the standard, and the values were found to be 0.72. These findings have proved that the employed method was specific, as it clearly separates the 4,4'-M(2,6-DTBP) compound from MEFM.

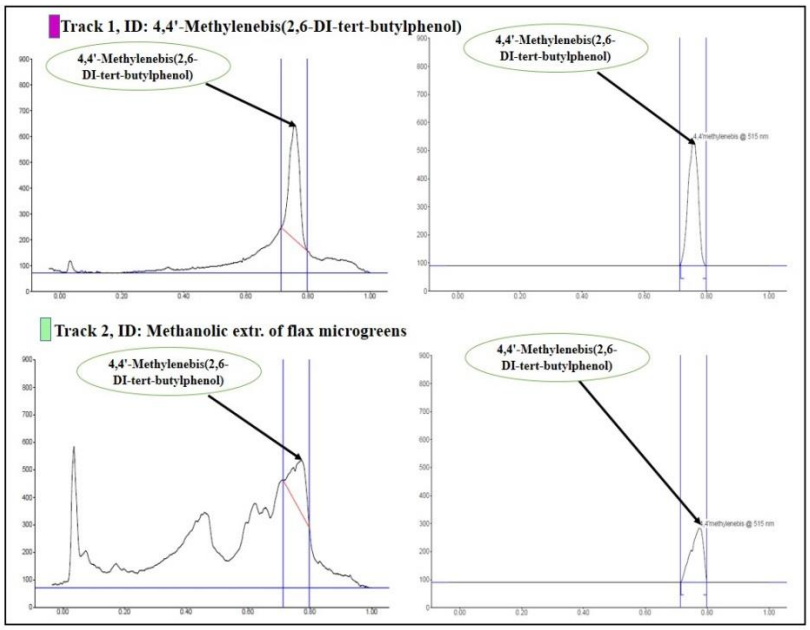

Fig. 2: Densitometry graph showing isolation of 4,4'-M(2,6-DTBP) from MEFM

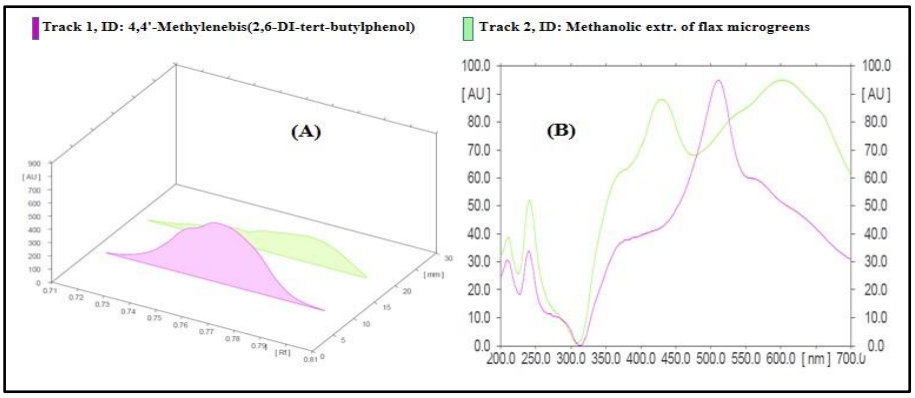

Fig. 3: (A) 3D Chromatogram of 4,4'-M(2,6-DTBP) from extract and standard. (B) Overlay of HPTLC chromatogram of all tracks

Table 2: HPTLC peak table of 4,4'-M(2,6-DTBP) and MEFM

Peak	Start Rf	Start height	Max Rf	Max height	Max %	End Rf	End height	Area	Area %	Assigned substance
1	0.72	11.0	0.76	446.3	100.00	0.80	0.40	14617.2	100.00	4,4'-M(2,6-DTBP)
1	0.72	2.3	0.78	196.5	100.00	0.80	12.3	7919.9	100.00	4,4'-M(2,6-DTBP)

In silico studies

Docking studies

The docking screening was done using the PyRx software [48]. Table 3 presents the docking result of 4,4'-M(2,6-DTBP) with PubChem ID (CID8372) against six prostate cancer drug targets: Aurora A kinase (AURKA), N-myc proto-oncogene protein (N-Myc), 5α-Reductase (5AR), Androgen receptor (AR), Lysine-specific histone demethylase 1A (LSD1), and Cluster of Differentiation 27 (CD27) as reported by Lawal *et al.* [18]. Throughout the docking result, the binding energies varied from −10.7 to −17.1 kcal./mol. According to the results, the ligand (CID8372) had binding energies of −15.8, −14.7, −10.7, −13.3, −17.1, and −14.9 kcal/mol for 5AR, AURKA, N-Myc, CD27, LSD1, and AR, respectively. CID8372 exhibits a maximum binding energy of −17.1 kcal/mol for LSD1. In comparison to flutamide (CID3397), a common medication for prostate cancer, had its highest binding energy of-10.5 kcal/mol for AR. CID8372 shows the highest binding energy, which was even more than CID11002708, CID290541, and AR inhibitors like enzalutamide [18, 49]. Also, the binding energy of CID8372 for 5AR is −15.8 kcal/mol, which is higher than that of finasteride (-9.8 kcal/mol) [50]. The higher binding energy of CID8372 as compared to standard drugs is because it forms strong H-bonds and more stable hydrophobic interactions with amino acid residues in the binding pocket of the target proteins, leading to more complex formation.

Half-maximal inhibitory concentration prediction

IC_{50} value is used as a measure of potency and how effective the compound inhibition is [51]. The predicted IC_{50} value for the CID8372 was in a range of 0.0003 to 14.80 nM (table 3). The 4,4'-M(2,6-DTBP) had shown the highest possible inhibitory potential with 0.0003 nM against the LSD1 target and the lowest possible inhibitory potential with 14.80 nM against the N-Myc target protein. In comparison to the control FDA drug, the 4,4'-M(2,6-DTBP) shows the predicted IC_{50} value higher than that of control FDA drugs.

Protein–ligand interactions of 4,4'-M(2,6-DTBP) against prostate cancer druggable targets

The mechanism of action of a drug can be studied through protein-ligand interaction analysis. There are various forces involved, including electrostatic, hydrogen, and hydrophobic bonds. Binding energy from docking results only cannot lead to a final conclusion [52]. In fact, the consideration of the amino acid residues that are part of the protein-ligand interaction improves the result of the docking and enhances the credibility of the findings. The findings demonstrate that at the active site of the target proteins, the amino acid residues interact favorably with the 4,4'-M(2,6-DTBP) molecule. The findings show that the enzyme possesses binding sites that can be occupied by this ligand; indeed, this is essential in drug design in which the enzyme activity can be inhibited (table 3). The result also demonstrates that the protein-ligand interaction made it more stable for the ligand to fit in the active site of the target proteins. A graphical representation of the protein-ligand interaction is shown as a 3D medium in fig. S2 (see supplementary material) [53, 54].

ADME/T properties prediction

ADMET lab 3.0 and ProTox-3.0 tools were used to assess the ADMET parameters for the 4,4'-M(2,6-DTBP) (CID8372). Table 4 presents the ADME results; the 4,4'-M(2,6-DTBP) compound has good oral bioavailability, blood-brain barrier (BBB) permeation, and high Gastrointestinal (GI) absorption. To estimate the effective bioavailability of 4,4'-M(2,6-DTBP), LRO5 and VR were applied. As per LRO5, phytocompounds with LogPo/w<5, molecular weight (MW)<500, number of hydrogen bond acceptors (n-HBA)<10, and number of hydrogen bond donors (n-HBD)<5 are likely to have good bioavailability [55]. The VR widens the criteria to include other additional parameters such as Topological Polar Surface Area (TPSA) ≤140 Å and number of rotatable bonds (n-ROTB)<10 [56]. The compound under study complied with the LRO5 and VR, and it showed favorable bioavailability. The ADMET analysis indicates that the 4,4'-M(2,6-DTBP) exhibits moderate BBB permeability. Despite it slow TPSA (40.46 $Å^2$) and moderate hydrogen bonding, this compound has limit passive diffusion and increase P-gp efflux due to its high molecular weight (424.66 g/mol) and excessive lipophilicity (LogP 7.306), reducing its overall BBB penetration. As compare to standard drugs, such as Diazepam (Valium) and Fluoxetine (Prozac) exhibits greater BBB penetration due to their lower molecular weights (284 g/mol and 309 g/mol), lower lipophilicity (LogP 2.82 and LogP 4.1), and lower TPSA values (32 $Å^2$ and 44 $Å^2$). These factors improved passive diffusion and CNS penetration, thus making them more potent for central nervous system (CNS) diseases.

As presented in table S2 in the supplementary material, the toxicity prediction study served to classify the 4,4'-M(2,6-DTBP) compound as class VI and presented no acute oral toxicity. This suggests that compound oral toxicity is very low, easily broken down, absorbed in the GIT, and transported to the target site. Also, this compound is non-neurotoxic, non-hepatotoxic, non-nutritional toxic, and non-carcinogenic. It also enhanced the biotransformation reactions by inducing cytochrome P450 (CYP450) enzyme and acted as a non-inhibitor of the CYP450 family. According to findings of Gilani and Cassagnol [57] and Deodhar *et al.* [58], it has been observed that any compound that inhibits most of the CYP450 enzyme family will block biotransformation, leading to decreased metabolism of drugs and increased potential toxicity. The proTox-3.0 prediction tool generated a toxicity radar graph to estimate the toxicity of a compound. The details about possible toxicity targets of 4,4'-M(2,6-DTBP) are presented in table S3 (see supplementary material). Compound therapeutic safety evaluation proved that it's safe and

possesses a broad range of therapeutic potentials (fig. S3; see supplementary material).

Table 3: Binding affinities, IC_{50} values, and interaction residues of 4,4'-M(2,6-DTBP) (CID8372) and FDA-approved drugs (Flutamide) across target proteins

Protein	CID8372 (kcal/mol)	Flutamide (kcal/mol)	CID8372 IC_{50}	Flutamide IC_{50}	CID8372-AA Residues	
					H-bond	Hydrophobic interactions
AURKA 4j8m)	-14.6	-8.4	0.021 nM	0.712 µM	ARG195B	PHE199B, PHE202B, TYR220B.
LSD1 *(*6 kgm)	-17.1	-10.2	0.0003 nM	0.034 µM	TYR81A	PRO61A, GLU62A, TYR81A, VAL85A, GLN86A, THR89B.
N-Myc (5G1X)	-10.7	-7.5	14.80 nM	3.245 µM	ASP555A	VAL333A, THR335A, PHE538A, LEU659A, TYR761A, ALA809A, THR810A.
5AR (7BW1)	-15.8	-9.4	0.0027 nM	0.132 µM	GLU57A, ASN193A.	TYR33A, TRP53A, TYR98A, ASN193A, PHE194A, PHE216A, PHE223A, LEU224A.
AR (3L3X)	-14.9	-10.5	0.012 nM	0.021 µM	CLY150A, CYS151A, THR152A, ALA154C.	LEU145C, PHE147A, HIS148B, THR152AB, ILE153A, ILE153C, ALA154B, ALA154C.
CD27 (7KX0)	-13.3	-8.6	0.180 nM	0.508 µM	LEU12A	LEU12A, ALA86B, THR89B, ILE117B.

Table 4: Drug-likeness, lipophilicity and physicochemical properties of CID8372

Compound ID	MW (g/mol)	TPSA	n-HBD	n-HBA	n-ROTB	M Ref	Log P	L. V	V. V	Pre. LD50 (mg/kg)
CID8372	424.66	40.46	2	2	6	137.02	7.306	0	0	24,000

Note. [a] MW: molecular weight (<500, expressed as Dalton); [b] TPSA: Topological polar surface area (Å2); [c] n-HBD: number of hydrogen bond donors (≤5); [d] n-HBA: number of hydrogen bond acceptors (≤10); [e] n-ROTB: number of rotatable bonds; [f] M Ref: molar refractivity; [f] LogP: logarithm of partition coefficient (<5) of compound between n-octanol and water; [g] LV: Lipinski's violation; [h] V. V= Veber's violation; [i] Pre. LD50: Predicted LD50.

In vitro analysis

Cell viability assay

The cytotoxicity effects of the MEFM, 4,4'-M(2,6-DTBP), and cisplatin (standard drug) against PC-3 were evaluated using the MTT assay (fig. 4), and the IC_{50} values were generated from dose-response curve studies. The MEFM exhibits strong cytotoxic activity against PC-3 cell lines, greater than the efficacy of the standard drug. The bioactive compound 4,4'-M(2,6-DTBP) exhibited weak bioactivity against PC-3 cell lines. The IC_{50} values for the MEFM and cisplatin were determined using nonlinear regression analysis, while 4,4'-M(2,6-DTBP) was calculated using linear regression analysis in Microsoft Excel. The IC_{50} values of MEFM, 4,4'-M(2,6-DTBP), and cisplatin were recorded as 377.5 µg/ml (95% CI: 377.48–377.52µg/ml; R^2 = 0.918), 2324.78 µg/ml (95% CI: 2324.74–2324.82µg/ml; R^2 = 0.9742), and 273.97 µg/ml (95% CI: 273.94–274.00µg/ml; R^2 = 0.9908), respectively, as presented in table 5. 4,4'-M(2,6-DTBP) indicated lower potency compared to MEFM and cisplatin. These results suggest that MEFM and cisplatin exhibit a more potent anticancer effect due to their nonlinear sigmoidal response, while 4,4'-M(2,6-DTBP) followed a linear response, requiring higher concentrations to achieve significant cytotoxicity. Even though 4,4'-M(2,6-DTBP) shows the highest binding affinity (-17.1 kcal/mol), it exhibits weak cytotoxicity, which is probably due to quick metabolism, low bioavailability, and poor cellular uptake. The reduced effectiveness may result from efflux via drug transporters, poor apoptosis activation, and the differences between *in silico* and *in vitro* conditions. Although it predicts strong target binding, actual intracellular interactions and biological responses may differ. The combination of the standard drug along with 4,4'-M(2,6-DTBP) will enhance cytotoxicity in PC-3 cell lines. Fig. 5 shows the MEFM, 4,4'-M(2,6-DTBP), and cisplatin-induced cellular shrinkage and damages the morphology of PC-3 cell lines. According to Kumari *et al.* [59], the cytotoxic activity is due to the apoptotic potential of the extract from *Pinus roxburghii*, a medicinal plant of Himachal Pradesh, making them potential candidates for therapeutic development in cancer treatment. According to the findings of Khan *et al.* [60], the *Moringa oleifera* methanolic leaves extract induces apoptosis and G0/G1 cell cycle arrest via downregulation of Hedgehog Signaling Pathway in human prostate PC-3 cancer cells.

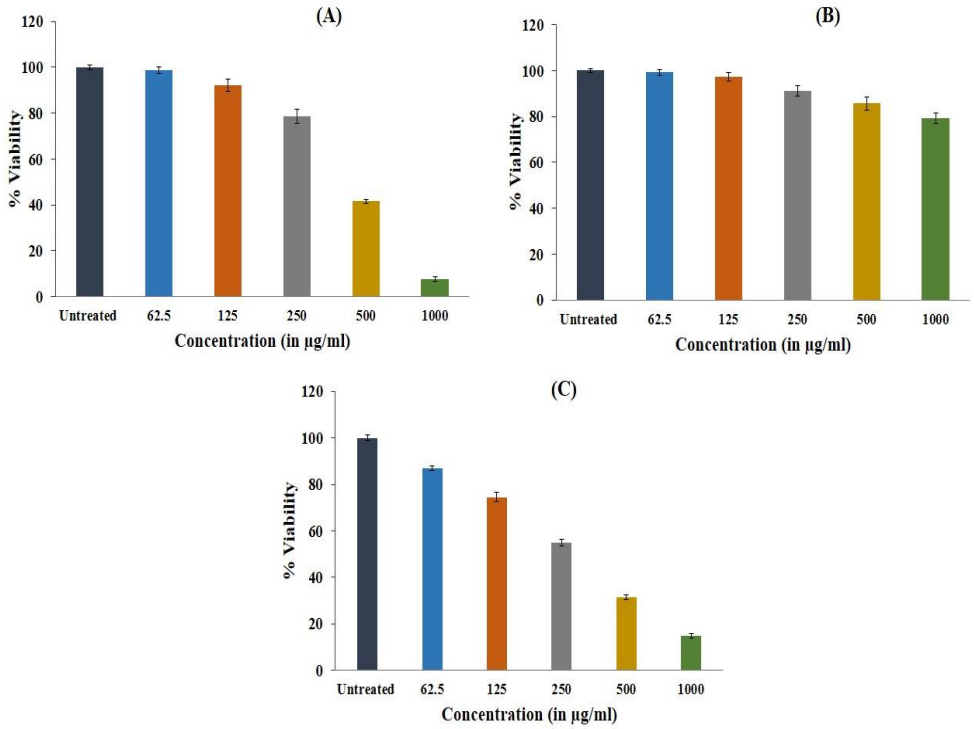

Fig. 4: MTT cell viability assay. Plot shows the percentage viability of PC-3 cells treated with (A) MEFM, (B) 4,4'-M(2,6-DTBP), and (C) Cisplatin (standard). Data are shown as the mean and standard deviation (mean±SD) of three replicates. mean **values (bar graphs), Standard deviation (vertical lines)**

Table 5: IC_{50} and CI values of cell proliferation inhibition of MEFM, 4,4'-M(2,6-DTBP), and cisplatin

PC-3 cell lines		
	IC_{50} (µg/ml)	**95% confidence interval (µg/ml)**
MEFM	377.5	377.48 – 377.52
4,4'-M(2,6-DTBP)	2324.78	2324.74 – 2324.82
Cisplatin	273.97	273.94 – 274.00

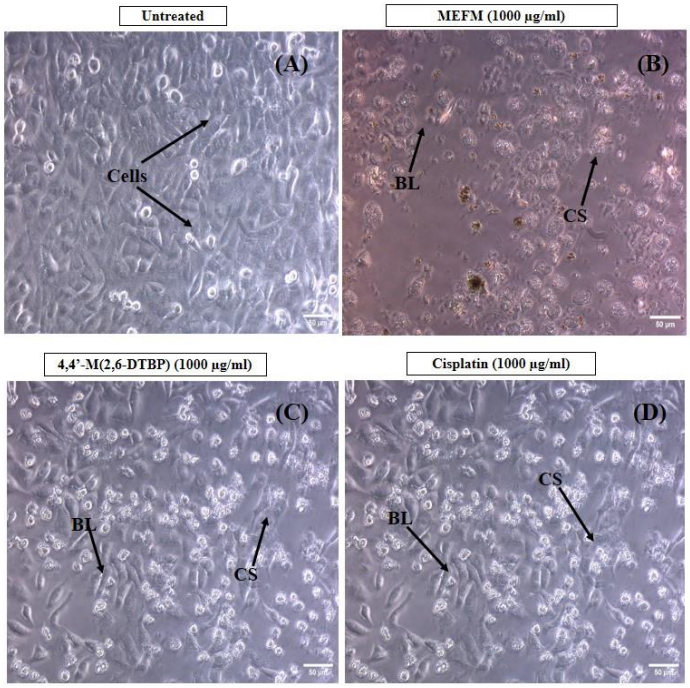

Fig. 5: Morphological changes in PC-3 cell lines at 24 h of treatment. (A) Untreated, (B) MEFM, (C) 4,4'-M(2,6-DTBP), and (D) Cisplatin. CS cellular shrinkage, BL membrane blebbing

Annexin apoptotic assay

To understand the mechanism of action of the MEFM and its bioactive compound, the annexin V apoptosis assay was performed. The apoptotic assay of the untreated MEFM, and 4,4'-M(2,6-DTBP) bioactive compound is presented in table 6. MEFM and 4,4'-M(2,6-DTBP) exhibited a significantly increased total apoptosis of 41.03 and 22.86%, respectively, compared to untreated cell lines (3.92%). In early apoptotic cells, the MEFM and 4,4'-M(2,6-DTBP) demonstrated significantly higher cell death (40.9 and 19.5, respectively), whereas in late apoptotic cells, the cell death was found to be 0.13 and 3.36%, respectively (table 6). Even though it indicates a significant level of cell death, its potency is lower compared to cisplatin, a standard PC-3 cell line's apoptotic inducer [61]. These findings indicate that this bioactive compound was highly effective in inducing cell death during the early apoptosis stage, but its efficiency in destroying cells decreased during the late apoptosis stage. Analysis of cell apoptosis of MEFM and 4,4'-M(2,6-DTBP) after 24 h incubation in PC-3 cell lines is depicted in fig. 6.

Table 6: Data showing the results in % of cells after MEFM and 4,4'-M(2,6-DTBP) treatment using annexin V apoptosis assay to identify its mechanism of action

Sample name	% of cells					Geometric mean fluorescence intensity (MFI) of Ab Flour 488 Annexin V (FL1-A parameter)
	Live	Early apoptotic	Late apoptotic	Debris	Total apoptosis	
Control (Untreated)	95.8	3.86	0.063	0.28	3.92	2002
MEFM	58.9	40.9	0.13	0.1	41.03	7934
4,4'-M(2,6-DTBP)	72.4	19.5	3.36	4.73	22.86	5620

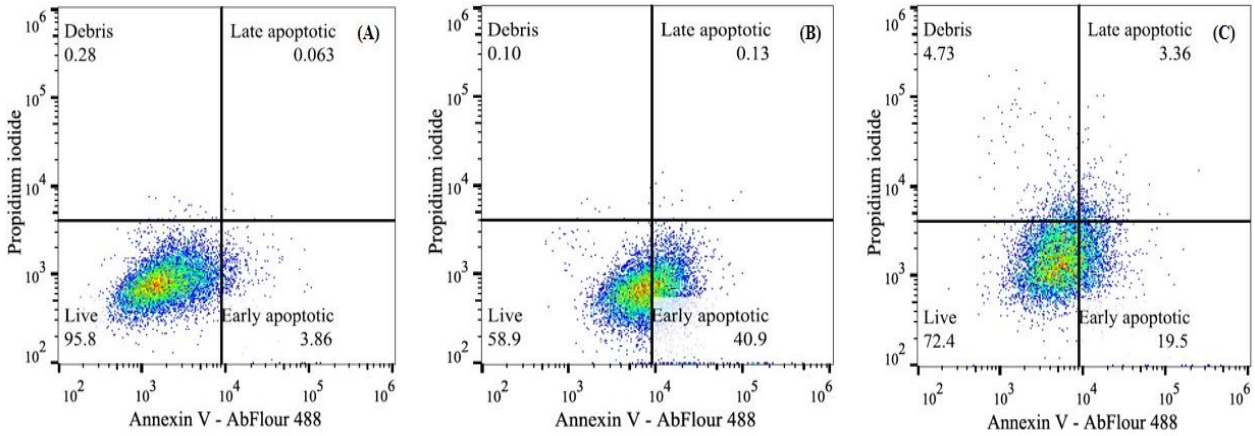

Fig. 6: **Plot showing Annexin V Apoptosis Assay results of (A) Untreated, (B) MEFM, (C) 4,4'-M(2,6-DTBP) treated PC-3 cells**

CONCLUSION

Conclusively, the flax microgreens contain numerous bioactive compounds with potential therapeutic importance, including anticancer properties. The plant extract demonstrated potent antioxidant activity through the DPPH assay and further analysis by HPTLC, which confirmed the presence of the 4,4'-M(2,6-DTBP) compound. The *in silico* studies revealed that this compound has the highest binding energy, good bioavailability, and low toxicity. In *in vitro* studies, MEFM showed strong anticancer activity; its bioactive compound exhibited weaker cytotoxicity, necessitating further optimization and combinatory studies (synergy testing with cisplatin or docetaxel). Further *in vivo* studies are required to evaluate their efficacy, metabolism, bioavailability, and toxicity in a living system.

ACKNOWLEDGEMENT

The authors thank the Dean of the School of Bioengineering and Biosciences in Lovely Professional University, Phagwara, Punjab, India.

FUNDING

Nil

ABBREVIATION

Methanolic Extract of Flax Microgreens (MEFM), 4,4'-Methylenebis (2,6-DI-tert-butylphenol) [4,4'-M (2,6-DTBP)], Gas Chromatography-Mass Spectrometry (GC-MS), High Performance Thin Layer Chromatography (HPTLC), 2,2-Diphenyl-2-Picryl-Hydrazyl (DPPH), 3-(4,5-Dimethylthiazol-2-yl)-2,5-Diphenyltetrazolium Bromide (MTT), Absorption, Distribution, Metabolism, Excretion, and Toxicity (ADMET), Surveillance, Epidemiology, and End Results (SEER), Alpha-linolenic acid (ALA), Prostate-Specific Antigen (PSA), 2,4-Di-tert-butyl-butyl phenol (2,4 DTBP), United Nations Sustainable Development Goals (UNSDGs), Dulbeccos Eagles Minimum Essential Medium (DMEM), Fetal Bovine Serum (FBS), Dimethylsulfoxide (DMSO), Phosphate Buffered Saline (PBS), Propidium Iodide (PI), Mass Spectrometry (MS), Institute of Standards and Technology (NIST), Retention Factor (Rf), 2D (2 dimensions), 3D (3 dimensions), Food and Drug Administration (FDA), Ligand Interaction Profiler (PLIP), Blood-Brain Barrier (BBB), Gastrointestinal (GI), Lipinski's Rule of Five (LRO5), Veber's rule (VR). National Centre for Cell Science (NCCS), Molecular Weight (MW), and Retention Time (RT), Aurora A Kinase (AURKA), N-Myc Proto-Oncogene Protein (N-Myc), 5α-Reductase (5AR), Androgen Receptor (AR), Lysine-Specific Histone Demethylase 1A (LSD1), and Cluster of Differentiation 27 (CD27), Topological Polar Surface Area (TPSA), Number of Hydrogen Bond Donors (n-HBD), Number of Hydrogen Bond Acceptors (n-HBA), Number of Rotatable Bonds (n-ROTB), Molar Refractivity (M Ref.), Logarithm of Partition Coefficient (LogP), Lethal Dose, 50% (LD50), Central Nervous System (CNS), Cytochrome P450 (CYP450).

AUTHORS CONTRIBUTIONS

All authors contributed to the study conception and design. ML took part in analyzing the experimental data, writing the methodology section, drafting the original, and visualization. Manuscript editing was done by IHK, VS, and GR. AKV assisted with the computational research. NRS provided assistance by critically reviewing the work. Supervision of the research work was done by GR, who also approved of the manuscript for publication. Each author has read and consented to the published document.

CONFLICT THE INTERESTS

There is no potential conflict of interest.

REFERENCES

1. Bergengren O, Pekala KR, Matsoukas K, Fainberg J, Mungovan SF, Bratt O. 2022 Update on prostate cancer epidemiology and risk factors a systematic review. Eur Urol. 2023 Aug 1;84(2):191-206. doi: 10.1016/j.eururo.2023.04.021, PMID 37202314.
2. Siegel RL, Giaquinto AN, Jemal A. Cancer statistics 2024. CA Cancer J Clin. 2024;74(1):12-49. doi: 10.3322/caac.21820, PMID 38230766.
3. Nweze C, Lay T, Muhammad A, Ubhenin A. Hypoglycemic hepatoprotective and hypolipidemic effects of pleurotus ostreatus in alloxan-induced hyperglycemic rats. TJNPR. 2017;1(4):163-7. doi: 10.26538/tjnpr/v1i4.5.
4. Stavropoulos P, Mavroeidis A, Papadopoulos G, Roussis I, Bilalis D, Kakabouki I. On the path towards a greener EU: a mini-review on flax (Linum usitatissimum L.) as a case study. Plants (Basel). 2023 Mar 1;12(5):1102. doi: 10.3390/plants12051102, PMID 36903961.
5. Nowak W, Jeziorek M. The role of flaxseed in improving human health. Healthcare (Basel). 2023 Jan 30;11(3):395. doi: 10.3390/healthcare11030395, PMID 36766971.
6. Imran S, Munir S, Altemimi AB, Fatima I, Rabail R, Batool I. Therapeutic implications of flaxseed peptides and bioactive components against various diseases. J Funct Foods. 2024 Aug 1;119:106324. doi: 10.1016/j.jff.2024.106324.
7. Mueed A, Shibli S, Jahangir M, Jabbar S, Deng Z. A comprehensive review of flaxseed (Linum usitatissimum L.): health affecting compounds mechanism of toxicity detoxification anticancer and potential risk. Crit Rev Food Sci Nutr. 2023 Dec 21;63(32):11081-104. doi: 10.1080/10408398.2022.2092718, PMID 35833457.
8. Krishnamoorthi R, Ganapathy AA, Hari Priya VM, Kumaran A. Future aspects of plant-derived bioactive metabolites as therapeutics to combat benign prostatic hyperplasia. J Ethnopharmacol. 2024 Aug 10;330:118207. doi: 10.1016/j.jep.2024.118207, PMID 38636573.
9. Rana A, Samtiya M, Dhewa T, Mishra V, Aluko RE. Health benefits of polyphenols: a concise review. J Food Biochem. 2022 Oct;46(10):e14264. doi: 10.1111/jfbc.14264, PMID 35694805.
10. Gasmi A, Mujawdiya PK, Noor S, Lysiuk R, Darmohray R, Piscopo S. Polyphenols in metabolic diseases. Molecules. 2022 Sep 23;27(19):6280. doi: 10.3390/molecules27196280, PMID 36234817.
11. Rudrapal M, Khairnar SJ, Khan J, Dukhyil AB, Ansari MA, Alomary MN. Dietary polyphenols and their role in oxidative stress-induced human diseases: insights into protective effects antioxidant potentials and mechanism(s) of action. Front Pharmacol. 2022 Feb 14;13:806470. doi: 10.3389/fphar.2022.806470, PMID 35237163.
12. Sharma A, Shahzad B, Rehman A, Bhardwaj R, Landi M, Zheng B. Response of the phenylpropanoid pathway and the role of polyphenols in plants under abiotic stress. Molecules. 2019 Jul 4;24(13):2452. doi: 10.3390/molecules24132452, PMID 31277395.
13. Samec D, Karalija E, Sola I, Vujcic Bok V, Salopek Sondi B. The role of polyphenols in abiotic stress response: the influence of molecular structure. Plants (Basel). 2021 Jan 8;10(1):118. doi: 10.3390/plants10010118, PMID 33430128.
14. Boyle TJ, Steele LA, Yonemoto DT. Synthesis and characterization of 4, 4′-methylenebis (2,6-di- tert -butylphenol) derivatives of a series of metal alkoxides and alkyls. J Coord Chem. 2012 Feb 10;65(3):487-505. doi: 10.1080/00958972.2012.654785.
15. Aravinth A, Perumal P, Rajaram R, Dhanasundaram S, Narayanan M, Maharaja S. Isolation and characterization of 2, 4-di-tert-butyl phenol from the brown seaweed dictyota ciliolata and assessment of its antioxidant and anticancer characteristics. Biocatal Agric Biotechnol. 2023 Nov 1;54:102933. doi: 10.1016/j.bcab.2023.102933.
16. Dalawai D, Murthy HN, Dewir YH, Sebastian JK, Nag A. Phytochemical composition bioactive compounds and antioxidant properties of different parts of andrographis macrobotrys nees. Life (Basel). 2023 May 11;13(5):1166. doi: 10.3390/life13051166, PMID 37240810.
17. Vargas Madriz AF, Kuri Garcia A, Vargas Madriz H, Chavez Servin JL, Ferriz Martinez RA, Hernandez Sandoval LG. Phenolic profile and antioxidant capacity of pithecellobium dulce (Roxb) Benth: a review. J Food Sci Technol. 2020;57(12):4316-36. doi: 10.1007/s13197-020-04453-y, PMID 33087946.
18. Lawal M, Sharma NR, Verma AK, Rakhra G. Molecular modeling and identification of flax microgreens lignans as novel prostate cancer target inhibitors. J App Biol Biotech. 2025;13(2):242-57. doi: 10.7324/JABB.2025.205522.
19. Hussen EM, Endalew SA. *In vitro* antioxidant and free radical scavenging activities of polar leaf extracts of Vernonia amygdalina. BMC Complement Med Ther. 2023 May 4;23(1):146. doi: 10.1186/s12906-023-03923-y, PMID 37143058.
20. Rajasree RS, Ittiyavirah SP, Naseef PP, Kuruniyan MS, Anisree GS, Elayadeth Meethal M. An evaluation of the antioxidant activity of a methanolic extract of *Cucumis melo L.* fruit (F1 hybrid). Separations. 2021 Aug 18;8(8):123. doi: 10.3390/separations8080123.
21. Ogoubi A, Evenamede KS, Kpegba K, Simalou O, Agbonon A. Phytochemical study and antioxidant antibacterial and antidiabetic activities of Flacourtia indica leaves extracts from the Togolese flora. Int J Pharm Pharm Sci. 2023 Aug 1;15(8):50-6. doi: 10.22159/ijpps.2023v15i8.48035.
22. Shaikh S, Badruddeen MIK, Irfan Khan M, Ahmed A. *In vitro* and *in vivo* screening of anti-inflammatory activity of methanolic and aqueous extracts of Anogeissus latifolia leaves. Int J Pharm Pharm Sci. 2022;14(11):65-72. doi: 10.22159/ijpps.2022v14i11.45593.
23. Mallard WG, Linstrom PJ. Editors. NIST chemistry WebBook. In: NIST standard reference database. Gaithersburg (MD): National Institute of Standards and Technology; 2008. Available from: https://webbook.nist.gov. [Last accessed on 19 Mar 2025].
24. Muhammad II, Pandey DK. HPTLC quantification of quercetin from leaf extracts of *C. occidentalis L.* and its inhibitory activity against protease enzyme of P. falciparum. Vegetos. 2024 Jun 11;37(5):1804-16. doi: 10.1007/s42535-024-00934-z.
25. Muhammad II, Pandey DK. A validated HPTLC quantification of artemisinin from different extracts of Artemisia annua L. and its inhibitory activity against serine hydroxyl methyltransferase (SHMT). J App Biol Biotech. 2024;12(6):1-10. doi: 10.7324/JABB.2024.178566.
26. Adhikari T, Ray PB, Saha P. Comparative study of quercetin content in marketed seeds of Linum usitatissimum L. (Flax) Salvia hispanica L. (Chia) and Helianthus annuus L. (Sunflower) and their microgreens using HPTLC from West Bengal. Ind J Pharm Edu Res. 2025;59(1s):s221-8. doi: 10.5530/ijper.20255309.
27. Adhikari T, Saha P. Quantitative estimation of immunomodulatory flavonoid quercetin by HPTLC in different leafy vegetables available in West Bengal. Pharmacogn Res. 2022;14(4):423-8. doi: 10.5530/Pres.14.4.62.
28. Verma AK, Gulati P, Lakshmi GB, Solanki PR, Kumar A. Interaction studies of gut metabolite; trimethylene amine oxide with bovine serum albumin through spectroscopic DFT and molecular docking approach. Biorxiv. 2023 Apr 6;4. doi: 10.1101/2023.04.06.535846.
29. Zulfat M, Hakami MA, Hazazi A, Mahmood A, Khalid A, Alqurashi RS. Identification of novel NLRP3 inhibitors as therapeutic options for epilepsy by machine learning based virtual screening molecular docking and biomolecular simulation studies. Heliyon. 2024 Aug 15;10(15):e34410. doi: 10.1016/j.heliyon.2024.e34410, PMID 39170440.
30. Lawal M, Verma AK, Umar IA, Gadanya AM, Umar B, Yahaya N. Analysis of new potent antidiabetic molecules from phytochemicals of pistiastrateotes with Sglt1 and G6pc proteins of homo sapiens for treatment of diabetes mellitus. An in silico approach. Silico approach. IOSR JPBS. 2020;15:59-73. doi: 10.9790/3008-1504025973.
31. Gulati P, Verma A, Kumar A, Solanki P. Para cresyl sulfate and BSA conjugation for developing aptasensor: spectroscopic methods and molecular simulation. ECS J Solid State Sci Technol. 2023;12(7):073004. doi: 10.1149/2162-8777/ace286.

32. Ogoubi A, Evenamede KS, Kpegba K, Simalou O, Agbonon A. Phytochemical study and antioxidant antibacterial and antidiabetic activities of Flacourtia indica leaves extracts from the Togolese flora. Int J Pharm Pharm Sci. 2023 Aug;15(8):50-6. doi: 10.22159/ijpps.2023v15i8.48035.
33. Baba H, Bunu SJ. Spectroscopic and molecular docking analysis of phytoconstituent isolated from solenostemon monostachyus as potential cyclooxygenase enzymes inhibitor. Int J Chem Res. 2025 Jan 1;9(1):1-6. doi: 10.22159/ijcr.2025v9i1.241.
34. Aiswariya, BV S, Satya MS. Molecular docking and admet studies of benzotriazole derivatives tethered with isoniazid for antifungal activity. Int J Curr Pharm Sci. 2022;14(4):78-80. doi: 10.22159/ijcpr.2022v14i4.2004.
35. Spackman PR, Turner MJ, McKinnon JJ, Wolff SK, Grimwood DJ, Jayatilaka D. CrystalExplorer: a program for hirshfeld surface analysis visualization and quantitative analysis of molecular crystals. J Appl Crystallogr. 2021 Jun 1;54(3):1006-11. doi: 10.1107/S1600576721002910, PMID 34188619.
36. Kumar S, Mohan A, Sharma NR, Kumar A, Girdhar M, Malik T. Computational frontiers in aptamer based nanomedicine for precision therapeutics: a comprehensive review. ACS Omega. 2024 Jun 10;9(25):26838-62. doi: 10.1021/acsomega.4c02466, PMID 38947800.
37. Ortiz CL, Completo GC, Nacario RC, Nellas RB. Potential inhibitors of galactofuranosyl transferase 2 (GlfT2): molecular docking 3D-QSAR, and in silico ADMETox studies. Sci Rep. 2019 Nov 19;9(1):17096. doi: 10.1038/s41598-019-52764-8, PMID 31745103.
38. Jha V, Dhamapurkar V, Thakur K, Kaur N, Patel R, Devkar S. In silico prediction of potential inhibitors for the M2 protein of influenza a virus using molecular docking studies. Asian J Pharm Clin Res. 2022;15(8):100-8. doi: 10.22159/ajpcr.2022.v15i8.44608.
39. Kaur B, Rolta R, Salaria D, Kumar B, Fadare OA, DA Costa RA. An in silico investigation to explore anti-cancer potential of foeniculum vulgare mill. phytoconstituents for the management of human breast cancer. Molecules. 2022 Jun 24;27(13):4077. doi: 10.3390/molecules27134077, PMID 35807321.
40. Mosmann T. Rapid colorimetric assay for cellular growth and survival: application to proliferation and cytotoxicity assays. J Immunol Methods. 1983 Dec 16;65(1-2):55-63. doi: 10.1016/0022-1759(83)90303-4, PMID 6606682.
41. Avadhoot Shastry R, Karur N, Habbu P, Daniel Madagundi S, Sangangouda Patil B, Hanumanthrao Kulkarni V. Pharmacognostical evaluation and *in vitro* cytotoxic activity of alcoholic and aqueous extracts of corm of Amorphophallus paeoniifolius (Dennst). RGUHS J Pharm Sci. 2021;11(4). doi: 10.26463/rjps.11_4_6.
42. Elasbali AM, Al Soud WA, Al Oanzi ZH, Qanash H, Alharbi B, Binsaleh NK. Cytotoxic activity cell cycle inhibition and apoptosis inducing potential of athyrium hohenackerianum (Lady fern) with its phytochemical profiling. Evid Based Complement Alternat Med. 2022;2022(1):2055773. doi: 10.1155/2022/2055773, PMID 35692581.
43. Shalal OS, Irayyif SM. Evaluation of cytotoxicity and apoptotic effects of Simarouba glauca on the prostate cancer cell lines PC3. J Pak Med Assoc. IQ-24. 2023 Sep 1;73(9):S113-8. doi: 10.47391/JPMA.
44. Chera EI, Pop RM, Parvu M, Soritau O, Uifalean A, Catoi FA. Flaxseed ethanol extracts antitumor antioxidant and anti-inflammatory potential. Antioxidants (Basel). 2022 Apr 30;11(5):892. doi: 10.3390/antiox11050892, PMID 35624757.
45. Girish YR, Sharath Kumar KS, Prashantha K, Rangappa S, Sudhanva MS. Significance of antioxidants and methods to evaluate their potency. Mater Chem Horiz. 2023 May 1;2(2):93-112. doi: 10.22128/mch.2023.647.1037.
46. Alachaher FZ, Dali S, Dida N, Krouf D. Comparison of phytochemical and antioxidant properties of extracts from flaxseed (Linum usitatissimum) using different solvents. Int Food Res J. 2018 Feb 1;25(1):75-82.
47. Hanaa MH, Ismail HA, Mahmoud ME, Ibrahim HM. Antioxidant activity and phytochemical analysis of flaxseeds (*Linumusitatisimum L.*). Minia J Agric Res Dev. 2017 Nov;37(1):129-40.
48. Saah SA, Sakyi PO, Adu Poku D, Boadi NO, Djan G, Amponsah D. Docking and molecular dynamics identify leads against 5 alpha reductase 2 for benign prostate hyperplasia treatment. J Chem. 2023;2023(1):1-20. doi: 10.1155/2023/8880213.
49. Ito Y, Sadar MD. Enzalutamide and blocking androgen receptor in advanced prostate cancer: lessons learnt from the history of drug development of antiandrogens. Res Rep Urol. 2018 Feb;10:23-32. doi: 10.2147/RRU.S157116, PMID 29497605.
50. Rao CM, Yejella RP, Rehman RS, Basha SH. Molecular docking based screening of novel designed chalcone series of compounds for their anti-cancer activity targeting EGFR kinase domain. Bioinformation. 2015;11(7):322-9. doi: 10.6026/97320630011322, PMID 26339147.
51. Cheng J, Hao Y, Shi Q, Hou G, Wang Y, Wang Y. Discovery of novel Chinese medicine compounds targeting 3CL protease by virtual screening and molecular dynamics simulation. Molecules. 2023 Jan 17;28(3):937. doi: 10.3390/molecules28030937, PMID 36770604.
52. Laskowski RA, Swindells MB. LigPlot+: multiple ligand protein interaction diagrams for drug discovery. J Chem Inf Model. 2011 Sep 15;51(10):2778-86. doi: 10.1021/ci200227u, PMID 21919503.
53. Rosario Ferreira N, Baptista SJ, Barreto CA, Rodrigues FE, Silva TF, Ferreira SG. In silico end to end protein ligand interaction characterization pipeline: the case of SARS-CoV-2. ACS Synth Biol. 2021 Nov 4;10(11):3209-35. doi: 10.1021/acssynbio.1c00368, PMID 34736321.
54. Dhiani BA, Nurulita NA, Fitriyani F. Protein protein docking studies of estrogen receptor alpha and TRIM56 interaction for breast cancer drug screening. Indones J Cancer Chemoprevent. 2022 Jun 28;13(1):46-54. doi: 10.14499/indonesianjcanchemoprev13iss1pp46-54.
55. Lipinski CA, Lombardo F, Dominy BW, Feeney PJ. Experimental and computational approaches to estimate solubility and permeability in drug discovery and development settings. Adv Drug Deliv Rev. 2001;46(1-3):3-26. doi: 10.1016/s0169-409x(00)00129-0, PMID 11259830.
56. Veber DF, Johnson SR, Cheng HY, Smith BR, Ward KW, Kopple KD. Molecular properties that influence the oral bioavailability of drug candidates. J Med Chem. 2002 Jun 6;45(12):2615-23. doi: 10.1021/jm020017n, PMID 12036371.
57. Gilani B, Cassagnol M. Biochemistry, cytochrome P450. In: Treasure Island, (FL): StatPearls Publishing; 2023. StatPearls. PMID: 32491630.
58. Deodhar M, Al Rihani SB, Arwood MJ, Darakjian L, Dow P, Turgeon J. Mechanisms of CYP450 inhibition: understanding drug drug interactions due to mechanism based inhibition in clinical practice. Pharmaceutics. 2020;12(9):846. doi: 10.3390/pharmaceutics12090846, PMID 32899642.
59. Kumari R, Saini AK, Kumar A, Saini RV. Apoptosis induction in lung and prostate cancer cells through silver nanoparticles synthesized from Pinus roxburghii bioactive fraction. J Biol Inorg Chem. 2020 Feb;25(1):23-37. doi: 10.1007/s00775-019-01729-3, PMID 31641851.
60. Khan F, Pandey P, Ahmad V, Upadhyay TK. Moringa oleifera methanolic leaves extract induces apoptosis and G0/G1 cell cycle arrest via downregulation of hedgehog signaling pathway in human prostate PC-3 cancer cells. J Food Biochem. 2020 Aug;44(8):e13338. doi: 10.1111/jfbc.13338, PMID 32588472.
61. Huang H, LI P, YE X, Zhang F, Lin Q, WU K. Isoalantolactone increases the sensitivity of prostate cancer cells to cisplatin treatment by inducing oxidative stress. Front Cell Dev Biol. 2021;9:632779. doi: 10.3389/fcell.2021.632779, PMID 33959604.